https://doi.org/10.15302/frontphys.2025.055204

RESEARCH ARTICLE

Epitaxy growth of centimeter-sized p-type monolayer molybdenum disulfide single crystals with high hole mobility

Yanan Peng[1], Xiaohui Li[1], Ling Huang[1], Junbo Yang[1], Hang Sun[1], Yinuo Li[1], Luying Song[1], Yulin Jiang[1], Zhu Du[1], Jun He[2], Jianping Shi[1,†]

[1] The Institute for Advanced Studies, Wuhan University, Wuhan 430072, China

[2] Key Laboratory of Artificial Micro- and Nano-Structures of Ministry of Education, School of Physics and Technology, Wuhan University, Wuhan 430072, China

Corresponding author. E-mail: †jianpingshi@whu.edu.cn

Received February 14, 2025; accepted April 7, 2025

Supporting Information

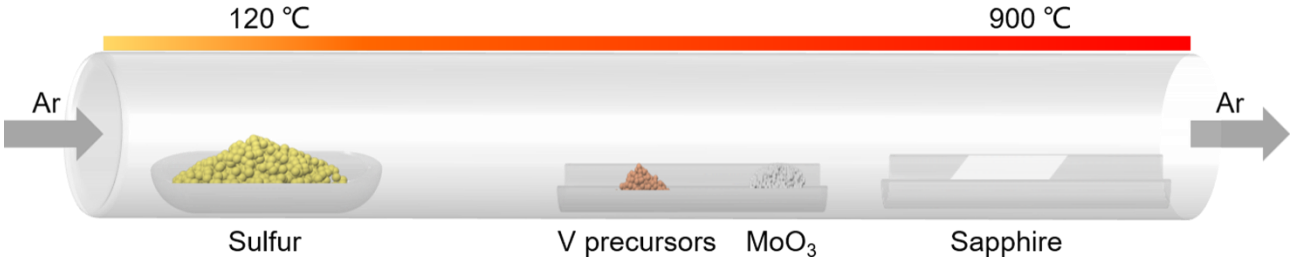

Fig. S1 Schematic diagram for CVD synthesis of monolayer V-MoS_2 single crystals on *c*-plane sapphire. The temperatures of S and MoO_3 powders are set to be 120 and 900 °C, respectively. The V precursors (V_2O_5, NH_4VO_3, and VCl_3) are placed at the middle of such two heating zones.

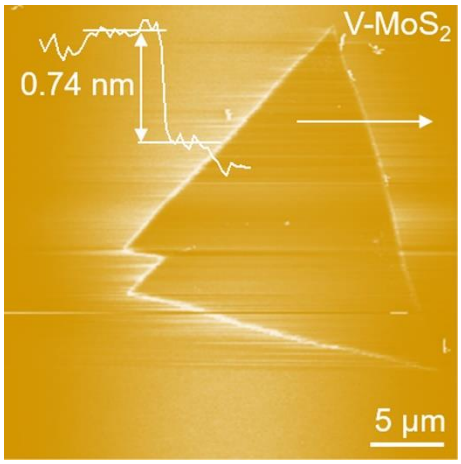

Fig. S2 AFM image and corresponding height profile analysis of as-grown V-MoS_2 nanosheets on *c*-plane sapphire, showing the monolayer feature.

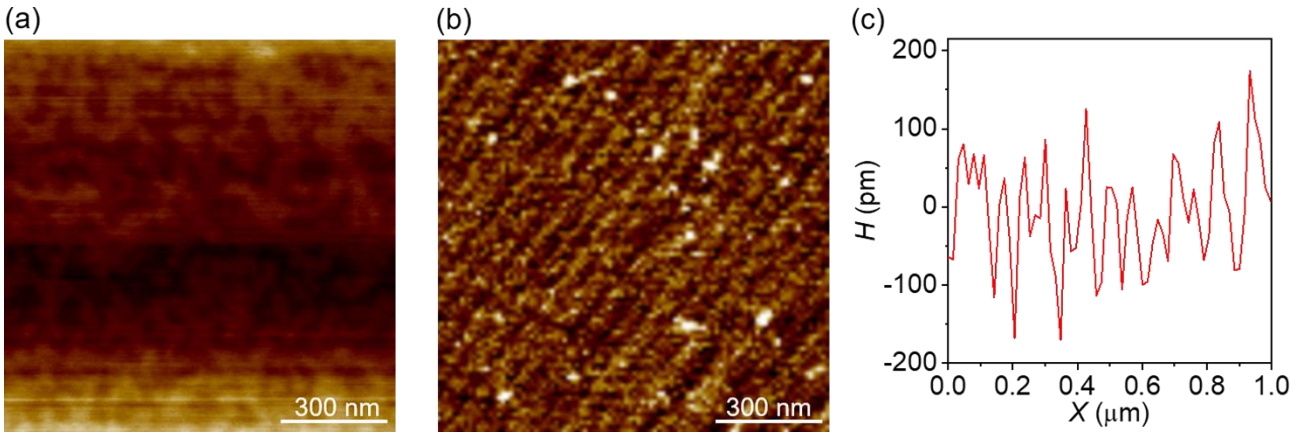

Fig. S3 (**a**) AFM image of *c*-plane sapphire before the CVD growth. AFM image (**b**) and corresponding height profile analysis (**c**) of *c*-plane sapphire after the CVD growth. The parallel steps with uniform and optimal heights are readily formed on sapphire surfaces with V assistance, which contribute to the edge-nucleation of unidirectionally aligned monolayer V-MoS_2 domains.

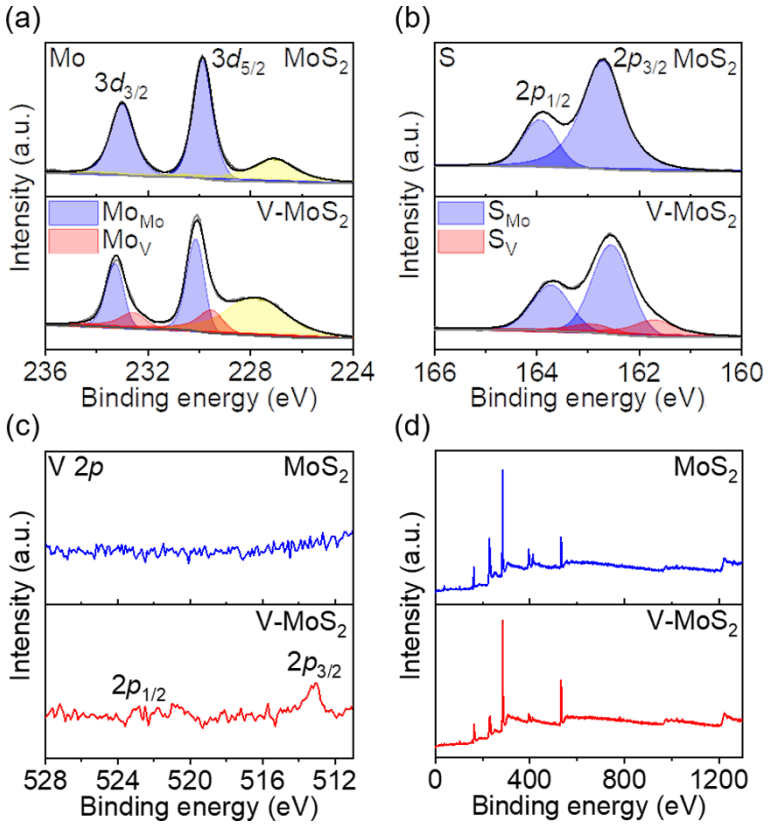

Fig. S4 XPS analyses of monolayer V-MoS_2 and pristine monolayer MoS_2. (**a**–**c**) High-resolution XPS spectra of Mo 3*d*, S 2*p*, and V 2*p* for monolayer V-MoS_2 and pristine monolayer MoS_2. Mo_V and S_V represent the Mo and S atoms whose bonding states are affected by the substituted V atoms. Mo_{Mo} and S_{Mo} represent the unaffected Mo and S atoms. (**d**) XPS full spectra of monolayer V-MoS_2 and pristine monolayer MoS_2.

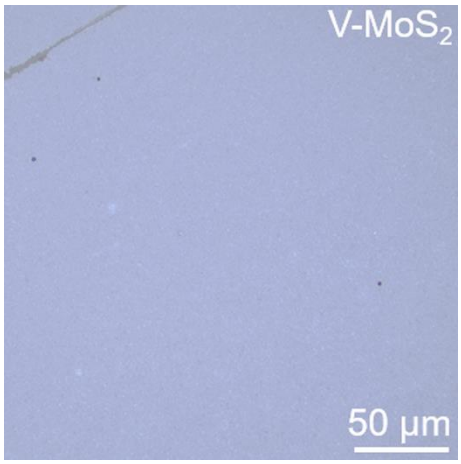

Fig. S5 OM image of as-grown monolayer V-MoS_2 single-crystal films on *c*-plane sapphire, showing the high thickness uniformity.

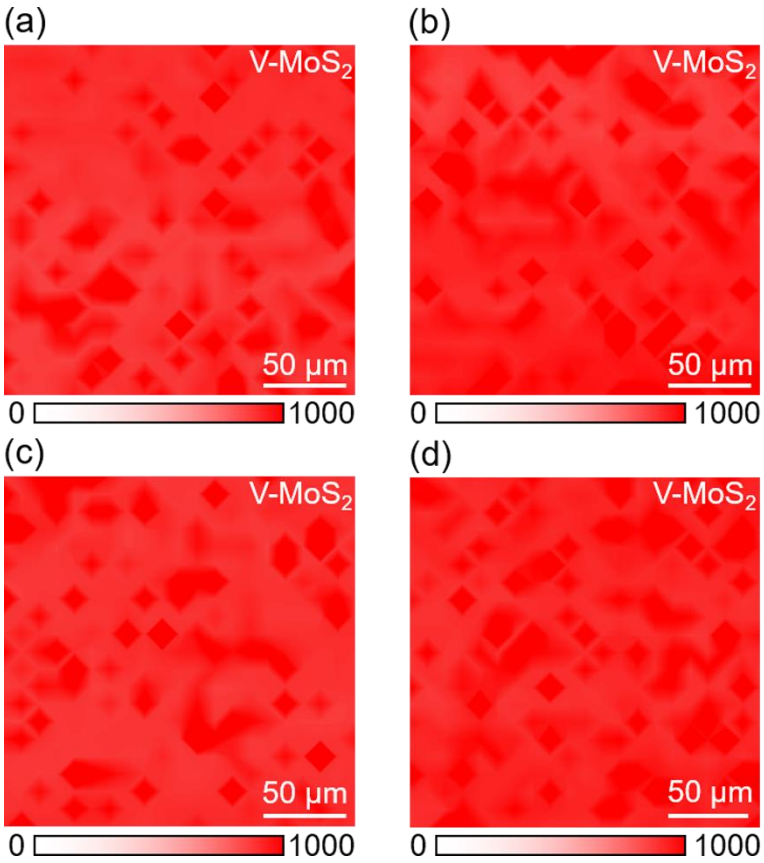

Fig. S6 The thickness uniformity and crystalline quality determination of large-area monolayer V-MoS_2 films. (**a**–**d**) Raman intensity mapping (A_{1g} mode) images captured from different areas of large-area monolayer V-MoS_2 single-crystal films.

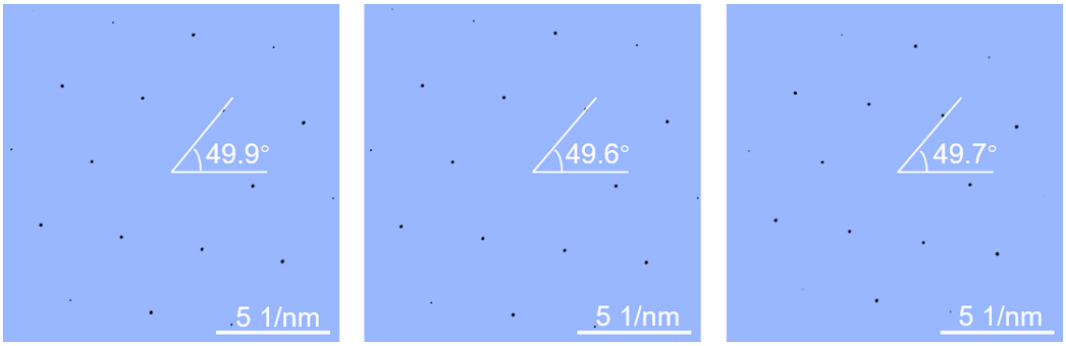

Fig. S7 SAED patterns captured from different areas of large-area monolayer V-MoS_2 films, revealing the nearly identical lattice orientations.

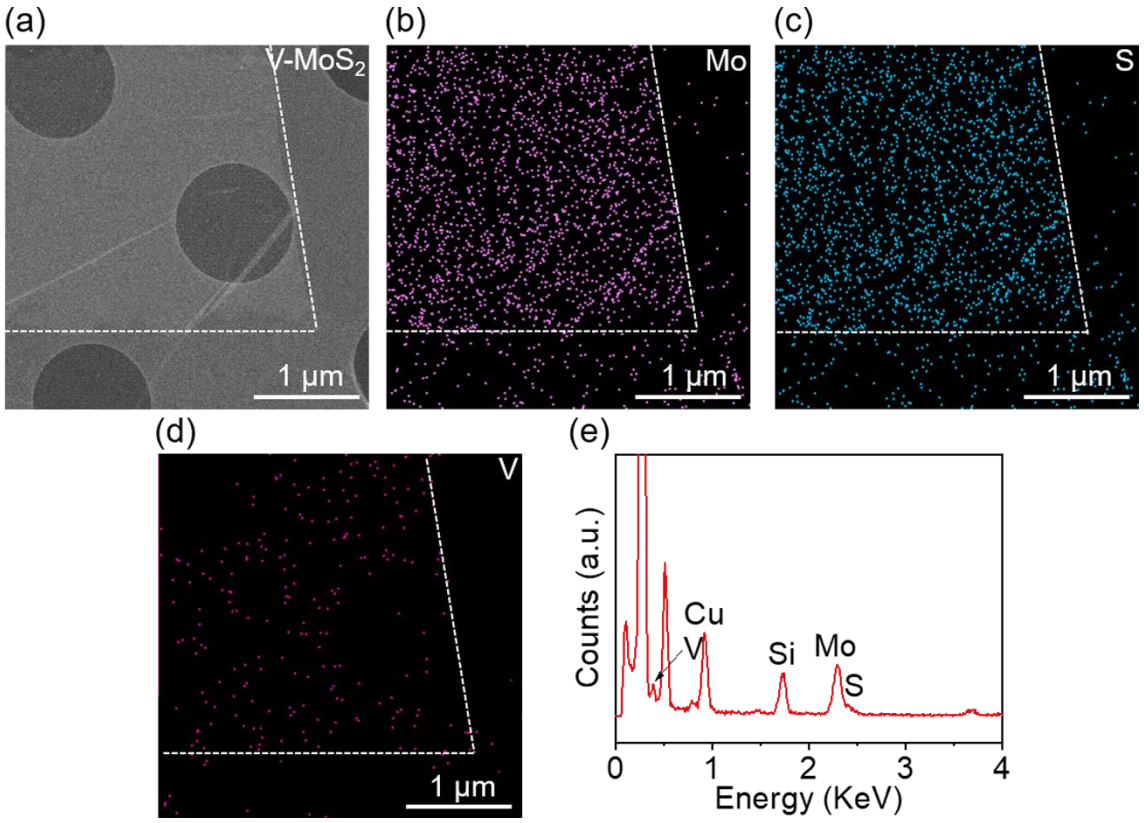

Fig. S8 The chemical constitution and distribution determination of monolayer V-MoS_2. (**a**) Low-magnification STEM image of a monolayer V-MoS_2 nanosheet. (**b**–**d**) EDS mapping images of Mo, S, and V elements, respectively. The uniform color contrast within the nanosheet suggests the high crystalline quality. (**e**) Quantified elemental analysis of monolayer V-MoS_2 and the V doping concentration is calculated to be 12.6 at%.

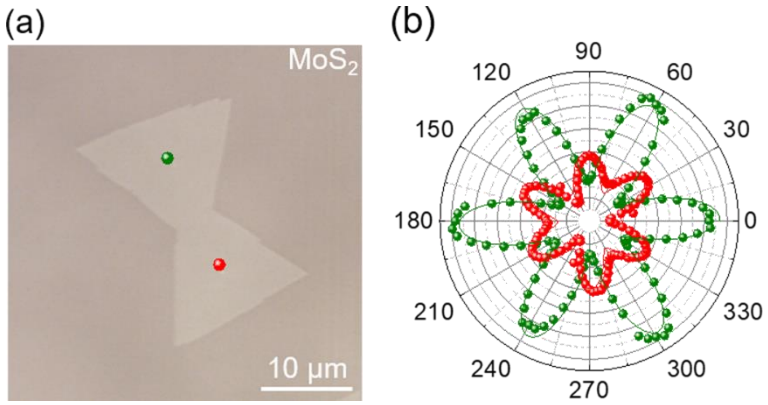

Fig. S9 The merging behavior of two monolayer MoS_2 nanosheets with different orientations. (**a**) OM image of two merged monolayer MoS_2 nanosheets with different orientations. (**b**) Corresponding polarized SHG spectra of such two monolayer MoS_2 nanosheets.

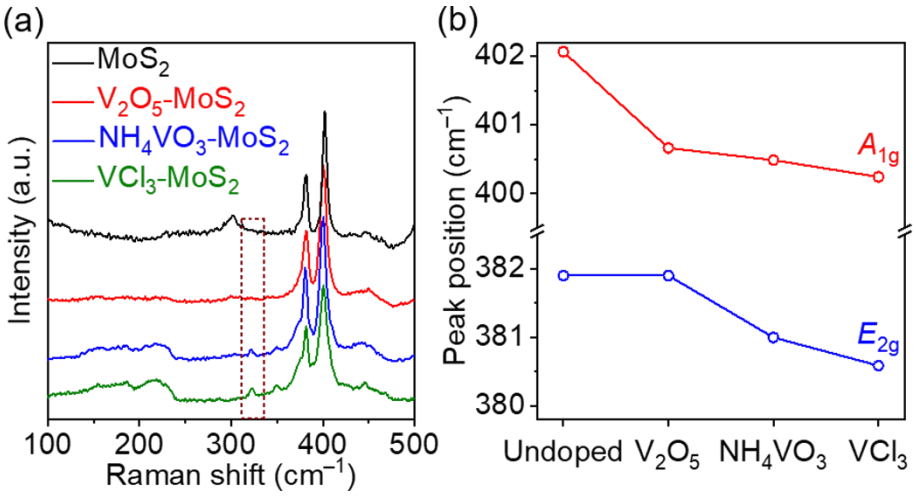

Fig. S10 Raman characterizations of monolayer V-MoS_2. Raman spectra (**a**) and the statistical data (**b**) of E_{2g} and A_{1g} peak positions for monolayer pristine MoS_2 and monolayer V_2O_5-, NH_4VO_3-, VCl_3-doped MoS_2.

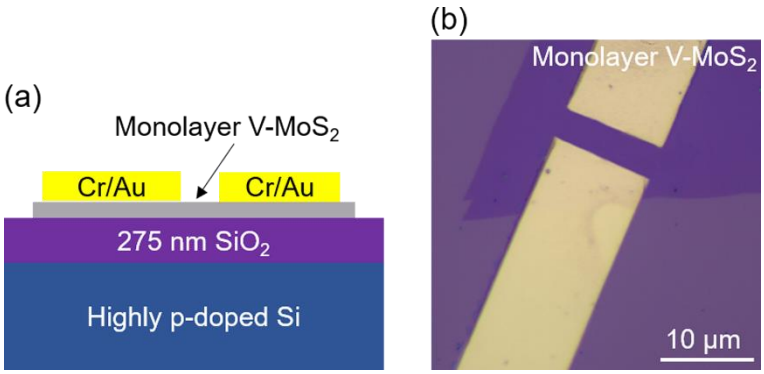

Fig. S11 The schematic diagram (**a**) and corresponding OM image (**b**) of monolayer V-MoS_2 back-gated FET.

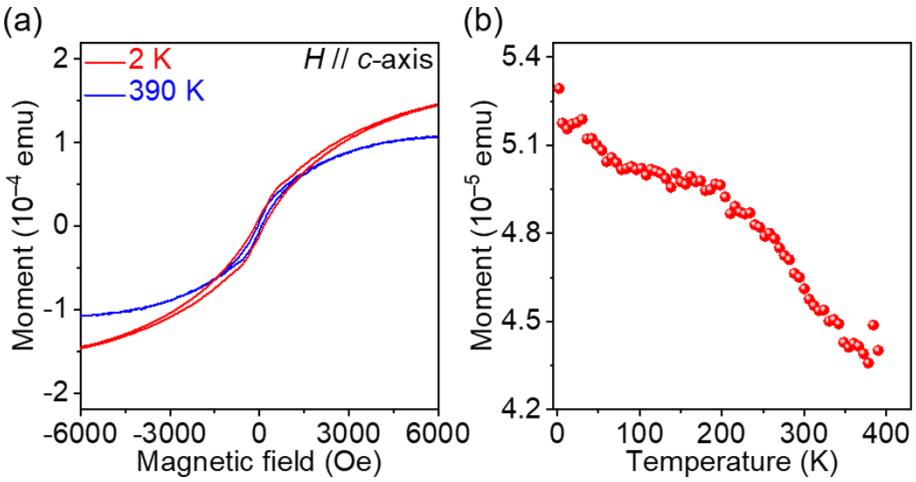

Fig. S12 Long-range ferromagnetic order in monolayer V-MoS_2. (**a**) Magnetic hysteresis loops of monolayer V-MoS_2 at the temperatures of 2 and 300 K with the magnetic field parallel to *c*-axis. (**b**) Plot of magnetic moment as a function of temperature.